

Structural characterization of plasma sprayed basalt–SiC glass–ceramic coatings

Ediz Ercenk^{a,*}, Ugur Sen^a, Senol Yilmaz^{a,b}

^a *Sakarya University, Engineering Faculty, Metallurgical and Materials Engineering Department, Esentepe Campus, 54187 Sakarya, Turkey*

^b *TUBITAK-MAM, Material Institute, 41470 Gebze, Kocaeli, Turkey*

Received 29 July 2010; received in revised form 14 September 2010; accepted 26 October 2010

Available online 1 December 2010

Abstract

In the present study, the effect of SiC addition on properties of basalt base glass–ceramic coating was investigated. SiC reinforced glass–ceramic coating was realized by atmospheric air plasma spray coating technique on AISI 1040 steel pre-coated with Ni + 5 wt.%Al bond coat. Composite powder mixture consisted of 10%, 20% and 30% SiC by weight were used for coating treatment. Controlled heat treatment for crystallization was realized on pre-coated samples in argon atmosphere at 800 °C, 900 °C and 1000 °C which determined by differential thermal analysis for 1–4 h in order to obtain to the glass–ceramic structure. Microstructural examination showed that the coating performed by plasma spray coating treatment and crystallized was crack free, homogeneous in macro-scale and good bonded. The hardness of the coated samples changed between 666 ± 27 and 873 ± 32 HV_{0.01} depending on SiC addition and crystallization temperature. The more the SiC addition and the higher the treatment temperature, the harder the basalt base SiC reinforced glass–ceramic coating became. X-ray diffraction analysis showed that the coatings include augeite [(CaFeMg)–SiO₃], diopside [Ca(Mg_{0.15}Fe_{0.85})(SiO₃)₂], albite [(Na,Ca)Al(Si,Al)₃O₈], andesine [Na_{0.499}Ca_{0.492}(Al_{1.488}Si_{2.506}O₈)] and moissanite (SiC) phases. EDX analyses support the X-ray diffraction analysis.

© 2010 Elsevier Ltd and Techna Group S.r.l. All rights reserved.

Keywords: D. Glass–ceramic; SiC; Plasma spray; Coating; Basalt

1. Introduction

Glass–ceramic materials are polycrystalline solids with a residual glassy matrix leading to a polycrystalline micro-structure that allows achievement of a better performance to abrasiveness and an increased resistance compared to traditional glasses [1]. Conventional glass–ceramics produced in two steps include nucleation and crystal growth. In general, the process is too expensive when the powder used in the process are technical grade oxide, besides the thermal treatments realized for the crystallization treatment of the glass form coating in the glass–ceramic coatings. But, natural volcanic rock powders can be used for glass–ceramic coatings without any nucleation agent and the process would be very cheaper than the glass–ceramics produced from pure oxides [2,3].

The basalt is a volcanic rock which is dark colored, small grain sized. Basalt covers more over than 2.5 billion km² of earth. Moreover, basalt fundamentally includes SiO₂, Al₂O₃, MgO, CaO and iron oxides (FeO, Fe₂O₃) in addition contain Na₂O, K₂O, P₂O₅, MnO and TiO₂ at small amount. Superior abrasion, wear and chemical resistant basalt-based glass–ceramics can be produced from the basalt [4].

Thermal spray is, in many cases, superior to other coating technologies with regard to process control and economic issues [5]. Plasma-sprayed ceramic coatings have been widely used for structural applications in order to improve resistances to wear, corrosion, oxidization, erosion, and heat [6]. Plasma spray processing can provide a reasonable method by which to prepare composite powders. Composite materials have the propensity to improve the mechanical, chemical and thermal behavior by combining materials with distinctive or supplementary properties [7].

In the present study, structural and mechanical properties of the glass–ceramics, produced from different compositions of the mixture of volcanic basalt rocks and SiC powders coated by

* Corresponding author. Tel.: +90 264 295 5791; fax: +90 264 295 5601.

E-mail address: ercenk@sakarya.edu.tr (E. Ercenk).

atmospheric plasma spray coating method and effects of the crystallization parameters, were investigated.

2. Experimental procedure

Basalt rocks obtained from Konya region of Turkey were chunked and crashed using jaw and conic crushers. It was milled using ring miller and sieved to the grids of -53 and $+45\text{ }\mu\text{m}$ for plasma spray coating. Basalt powders used in the coating process were analyzed using Perkin-Elmer 2300 atomic absorption spectroscopy. The chemical compositions of the basalt powders used in the study were given in Table 1. SiC was used as reinforced materials the average particle size of which was $-53\text{ }\mu\text{m}$. AISI 1040 steel was used as a substrate material in the dimensions of 20 mm in diameter and 5 mm in height. Steel samples were cleaned in ethyl alcohol and acetone, ultrasonically for 15 min and then sand blasted with 35 grit alumina. The resulting average roughness of the substrate surface (Ra) after grid blasting that measured Perthometer M4P surface roughness tester is between 3.5 and 4.6 μm . Also, these samples were cleaned again in ethyl alcohol and acetone for 15 min and dried. Ni–5 wt.%Al (METCO 450 NS) was used for the bond coat layer. The torch nozzle used for coatings was METCO 3 MB with 6 mm alloyed Cu nozzle. The position of the injector relative to the nozzle exit was 90° . The injector is in the same axis with torch. Powder unit of injector was METCO 3 MP powder feed unit. The coating operations were performed in the room temperature.

Basalt powder was mixed with 10%, 20% and 30% SiC powder by weight in the rotating chamber for homogenous mixing of the composite powders. Specific masses of SiC and basalts in the powder mixtures are 0.20, 0.42, 0.66 and 0.80, 0.58, 0.34 g/cm^3 , respectively. Atmospheric plasma spray coating technique was used for coating treatment of the prepared composite powder on bond coated steel samples. Plasma spray coating parameters used in the coating treatment was shown in Table 2. Differential thermal analysis (DTA) was performed on the coated samples for determining the crystallization temperature with heating rate of $15\text{ }^\circ\text{C min}^{-1}$ up to $1000\text{ }^\circ\text{C}$ temperature using TA instrument thermal analysis device. Coated samples were controlled heat treated for crystallization to produce glass–ceramic coatings at $800\text{ }^\circ\text{C}$, $900\text{ }^\circ\text{C}$ and $1000\text{ }^\circ\text{C}$ in argon atmosphere by a Protherm tube furnace with a time ranging from 1 to 4 h to promote internal

Table 2

Plasma spray coating parameters.

Coating parameter	Value
Plasma gun (MB)	3
Current (A)	500
Voltage (V)	64–70
Gas flow for Ar (l/min)	50
Gas flow for H (l/min)	15
Spray distance (mm)	130
Powder feed rate (g/min)	39
Carrier gas flow (l/min)	3–6

crystallization. Fig. 1 shows the flow chart of SiC reinforced basalt based glass–ceramic coating process. JEOL 6060 scanning electron microscopy (SEM) with energy dispersive X-ray spectroscopy (EDX) and X-ray diffraction analysis (XRD) using Rigaku type diffractometer with a $\text{CuK}\alpha$ radiation, which has a wavelength of $1.54056\text{ }\text{\AA}$ to analyze phases present in the coatings over a 2θ range of $10\text{--}90^\circ$ were used for characterization of the coated samples. XRD analysis was also performed for basalt rock. The hardness of basalt-based coating layer was measured on the cross-sections using a Future tech FM 700 Vickers indenter with a load of 10 gf.

3. Results and discussion

Fig. 2 shows XRD analysis of basalt rock. It was found that the main crystalline phases were albite $[(\text{Na,Ca})\text{Al}(\text{Si,Al})_3\text{O}_8]$, anorthite $[\text{Ca}(\text{Al}_2\text{Si}_2\text{O}_8)]$, augite $[(\text{CaFeMg})\text{--SiO}_3]$ and diop-

Table 1
Chemical composition of the basalt powder.

Compounds	wt. %
SiO_2	45.88
Al_2O_3	18.2
Fe_2O_3	9.95
CaO	9.28
MgO	6.62
K_2O	1.64
Na_2O	4.76
P_2O_5	1.04
LOI	2.63

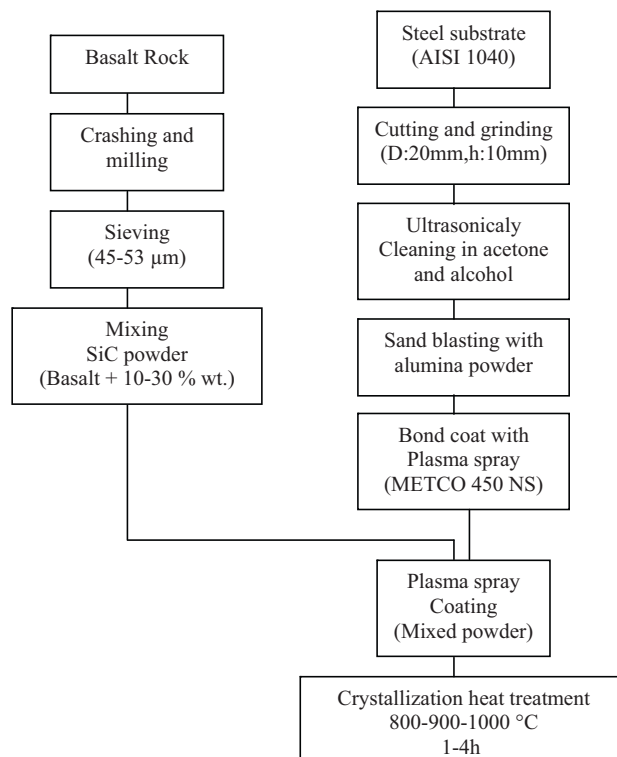


Fig. 1. Flow chart of SiC reinforced basalt based glass–ceramic coating process.

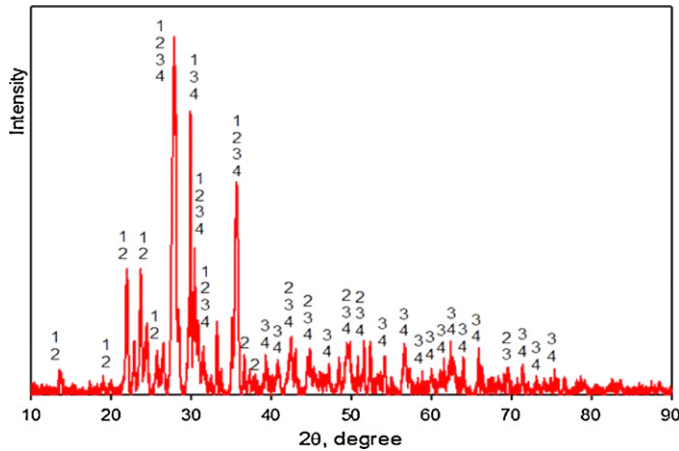


Fig. 2. XRD analysis of basalt (1. Albite, 2. Anorthite, 3. Augite, 4. Diopside).

side $[\text{Ca}(\text{Mg}_{0.15}\text{Fe}_{0.85})(\text{SiO}_3)_2]$. These phases are common for basalt rock as reported by the literature [8,9].

SEM cross and surface sectional examinations of basalt-based SiC reinforced glass–ceramic coating on AISI 1040 steel

with Ni–5%Al bond coat were shown in Fig. 3. The average thicknesses of bond coating and coating layers were $51 \pm 9 \mu\text{m}$ and $218 \pm 37 \mu\text{m}$, respectively. At the high magnifications (see Fig. 3(a)), three distinct regions were identified on the cross-sections of the coated sample: these are: (i) basalt base SiC reinforced coating layer, (ii) Ni–5 wt%Al (METCO 450 NS) bond coat between basalt base SiC reinforced coating layer and (iii) AISI 1040 steel matrix. Thermal expansions of AISI 1040 steel and basalt coating are $11.3 \times 10^{-6} \text{ } ^\circ\text{C}^{-1}$ and $5.1 \times 10^{-6} \text{ } ^\circ\text{C}^{-1}$, respectively [8,10]. Because of mismatch in both mechanical and thermal properties between coating and underlying substrate material, such coatings are often subjected to environments in which cracking, spalling and delamination may occur, often with potentially disastrous results [3,11]. It was observed that the coating layer was comparatively dense and homogeneous (Fig. 3(b)). However, basalt coating layer contains some inhomogeneities including porosity and a few semi-melted particles.

Fig. 4 shows the scanning electron micrograph and EDX analyses of the fractured surface of the coated sample. SiC particle was clearly determined on the fracture surface. In

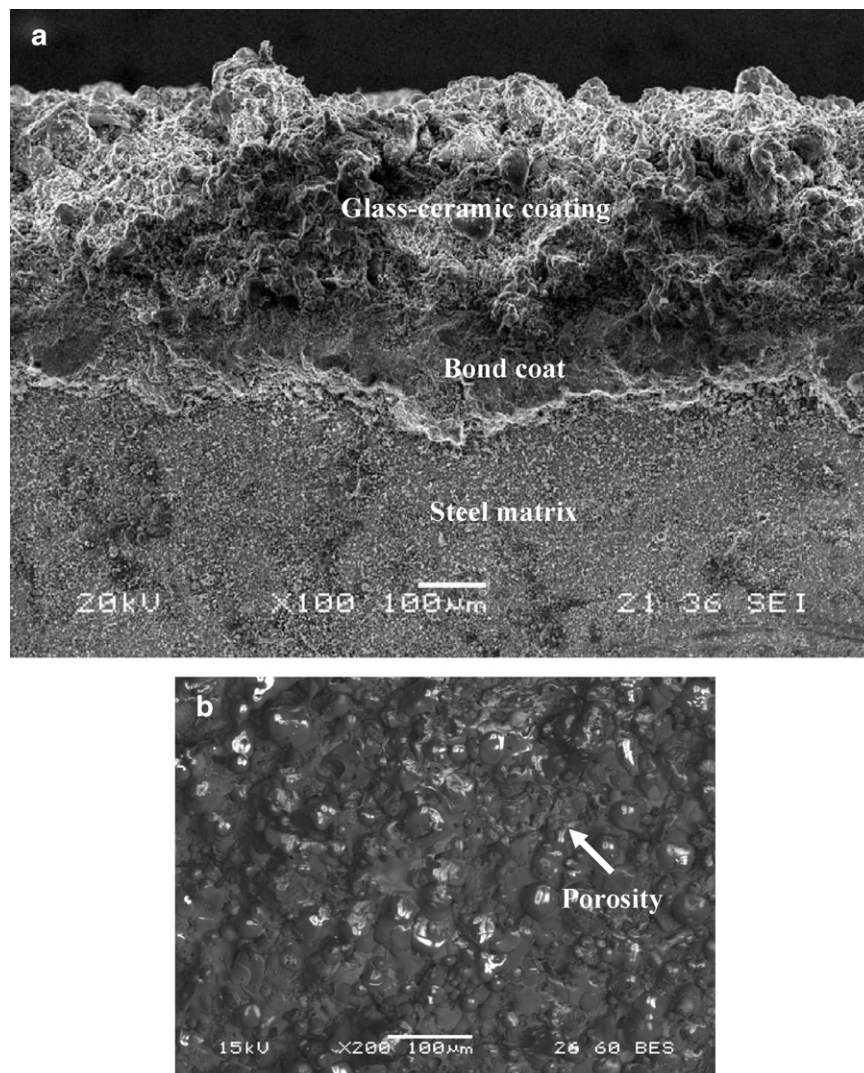


Fig. 3. SEM microstructure of %10 SiC reinforced glass–ceramic coating with 800 °C for 2 h. (a) Cross section of the coating; (b) surface section of the coating.

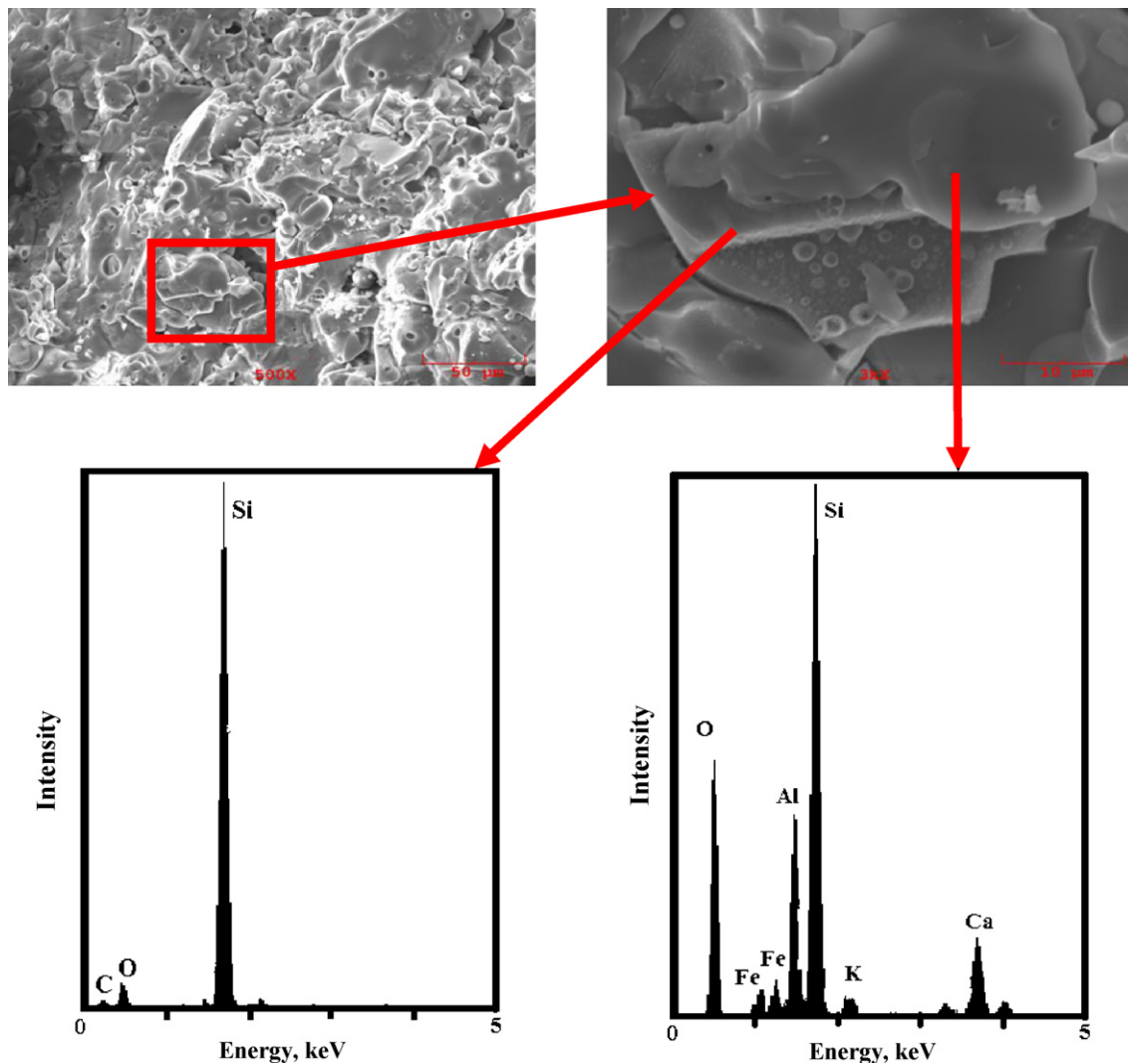


Fig. 4. SEM micrograph and EDS analyses of %10 SiC reinforced glass-ceramic coating with 800 °C for 2 h.

general, SiC particles in the microstructure of SiC reinforced basalt base glass-ceramic coating cannot be determined. Probably, the SiC particles were melted in the plasma flame and melted particles were oxidized in the atmospheric conditions. Thereby, SiC was surrounded with SiO₂ (glass form). The results agree with Bartuli et al. [12] and Sevostyanov et al. [13].

X-ray diffraction analysis of the 0%, 10%, 20% and 30% SiC reinforced basalt base glass-ceramic coatings heat treated at 900 °C for 2 h and without heat treatment were shown in Fig. 5. The XRD pattern shows that (Fig. 5(a)), coatings were amorphous and includes some small crystalline phase peaks originating from unmelted particles in the plasma spray coating treatment. SiC peaks are not determined by XRD analysis in coatings after plasma spray operation. SiC was surrounded with SiO₂ (glass form) [12,13] as seen in SEM micrographs (Fig. 4).

Plasma spray coating technique can be used for glass coating from the crystalline oxide-based ceramics which are suitable for glass formation [3,14,15]. As it is known that, amorphous glass structure is necessary for glass-ceramic production prior to the crystallization heat treatment [3,8,16]. As it can be seen

in Fig. 5(b), crystallization degree of the coating layer is changing depending on SiC addition percentage. The phases formed in the glass-ceramic coating after crystallization heat treatments are includes augite, diopside, albite, andesine and moissanite phases which are confirmed by XRD analysis. As it can be seen, the more the SiC addition resulted in the higher the crystalline peak intensities and the lower the background XRD pattern. It is probably that the more the SiC addition caused the more heterogeneous nucleation surfaces. As known, heterogeneous nucleation can be the precursor to devitrification of glass if the foreign particles are brought in to contact with the glass under conditions where they would not be dissolved. In the glass-ceramics, increase in the nucleation agents added increases the crystallization degree of the glass-ceramics [16].

Fig. 6 presents the microhardness of SiC reinforced basalt-based glass-ceramic coatings depending on SiC addition (0–30 wt.%) and treatment temperature (800–1000 °C for 2 h) in the form of contour diagrams. The Vickers microhardness results were between 666 ± 27 and 873 ± 32 HV_{0.01} (Fig. 6(a)). The highest hardness values were observed at %30 SiC additives as expected. It can be appeared that hardness

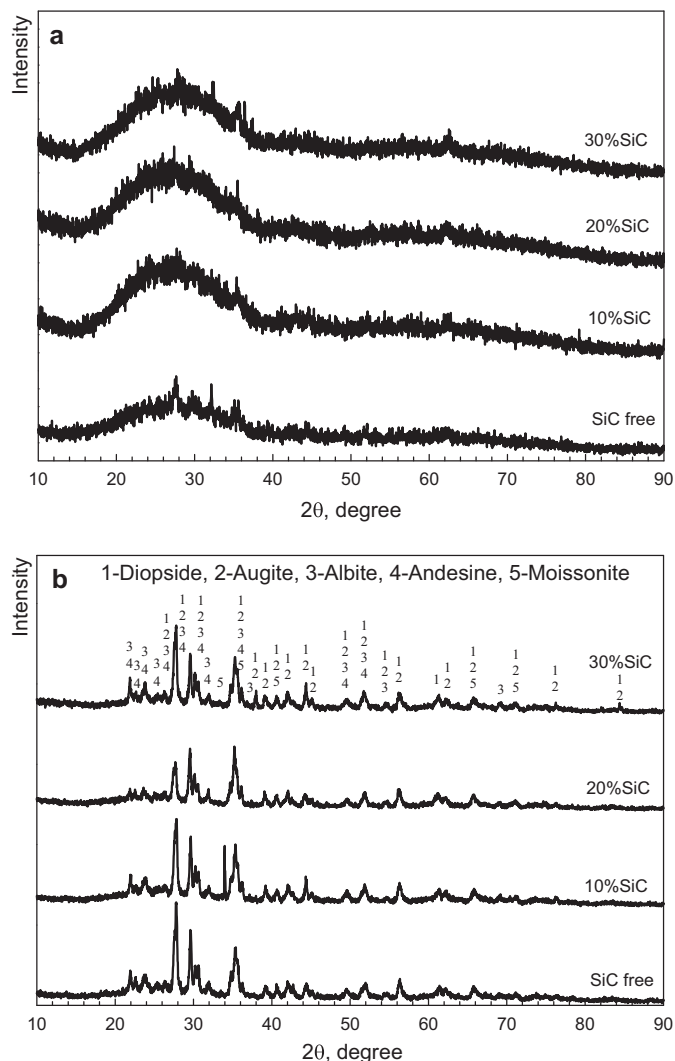


Fig. 5. XRD analysis of coatings; (a) before crystallization (b) after crystallization.

values generally increase till 1000 °C. Analysis showed that the hardness of the coating layer increases with increasing heat treatment temperature and SiC addition. Increasing in hardness is the result of existence of SiC particles as a barrier to plastic deformation of glass and glass–ceramic matrix under the load. Not only existing of particles in coatings increases hardness of SiC reinforced basalt base glass–ceramic coating, but also heat treatment can improve the hardness of these composite deposits whereas maximum value of hardness (873 HV_{0.01}) has been obtained in heat treated composite coating at 1000 °C.

It is possible to predict the SiC reinforced basalt base glass–ceramic coating hardness depending on the SiC addition and treatment temperature from Fig. 6(b). The contour diagram can be used for two purposes: (a) to predict the hardness of the coating with respect to the process parameters, i.e. SiC addition and treatment temperature; (b) to determine the value of process temperature and SiC addition for obtaining a predetermined coating layer hardness [17]. The hardness of bond coat and steel substrate used in this study are 215 ± 16 and 132 ± 14 HV_{0.01}, respectively. It is clear that the hardness of SiC reinforced

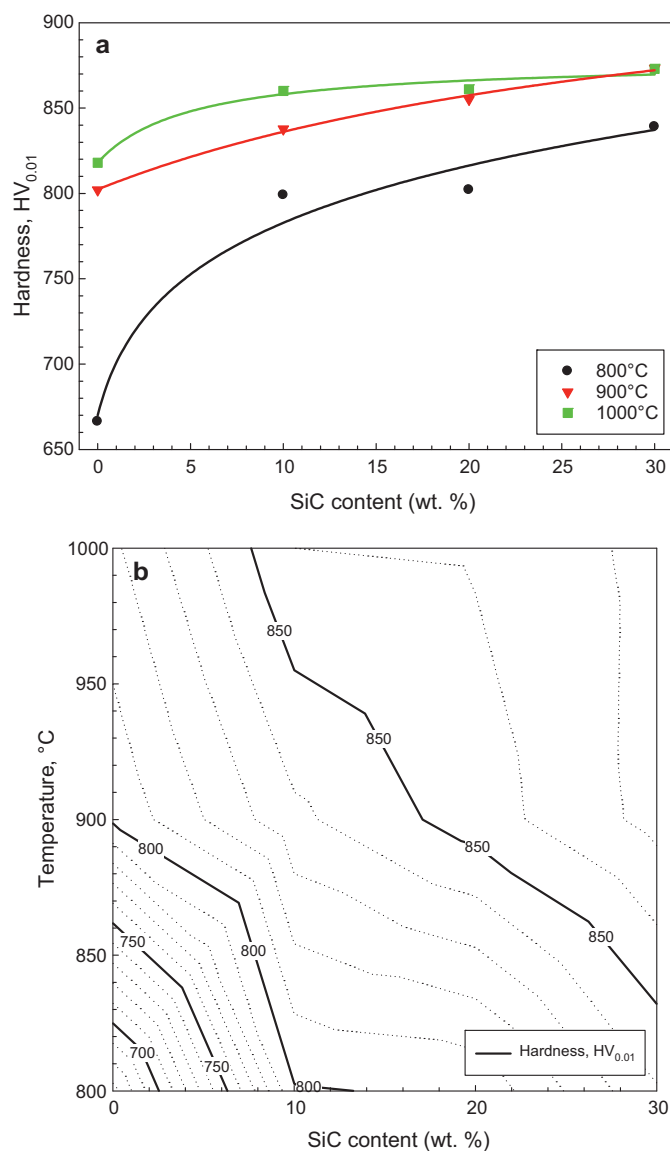


Fig. 6. Vickers microhardness for coatings (crystallization time: 2 h); (a) hardness graph (b) contour diagram.

basalt-based glass–ceramic coating is much higher than that of steel matrix and bond coat.

DTA studies were performed on the glassy coatings to determine the crystallization temperature with heating rate of 15 °C min^{-1} up to 1000 °C. DTA curves of coated basalt glass show a small endothermic peak (the glass transition temperature, T_g) and two exothermic peaks indicating the crystallization (Fig. 7) whatever SiC addition. The appearance of two and more crystallization peaks (T_p) on the DTA curve implies that at least two and more different crystal phases are formed during the heat treatment. This was also confirmed by XRD results (Fig. 5). This agrees with in previous studies [3,8]. The crystallization temperatures given in the experimental procedure were selected from the DTA curve depending on the endothermic and exothermic reaction temperatures. The glass transition (T_g) and crystallization (T_p) temperatures are given in Table 3. The more the SiC addition resulted in the lower glass transition temperatures. It is possible that the unmelted SiC

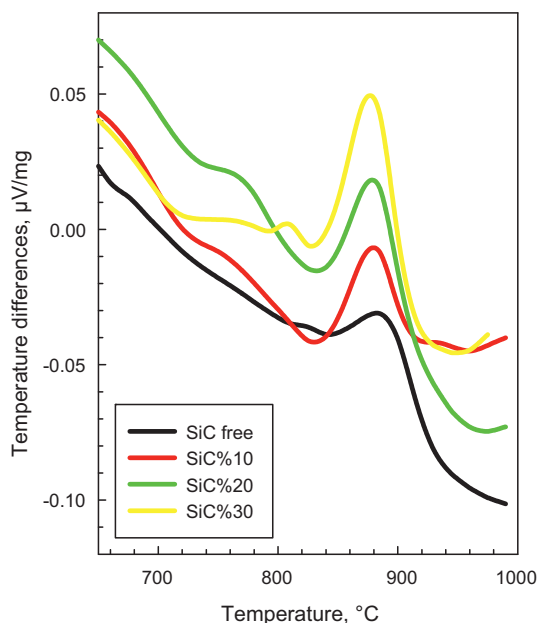


Fig. 7. DTA curves of %10 SiC reinforced glass–ceramic coating 15 °C/min.

Table 3

DTA measurements of plasma spray coated basalt base glass with/without SiC addition.

SiC addition (wt.%)	Peak temperatures, °C			
	T_g	T_{p1}	T_{p2}	T_{p3}
0	806	820	882	–
10	731	753	879	–
20	733	759	879	–
30	718	759	807	876

particles have the heterogeneous nucleation agent role as shown from the T_g temperatures of DTA curves depending on SiC addition (Fig. 7), but no remarkable effect on the crystallization temperatures of the glasses. As known SiC particles in the powder mixtures can be oxidized during the coating process and mix with melted basalt particles, so the chemical compositions of the coated glass very close to each other. For this reason, T_p temperatures of the coated glasses in the period of crystallization process are very similar. Already, the glass crystallization peak temperature, T_p , is high or low does not mean that the glass crystallization is difficult or easy [18].

4. Conclusions

The following results can be drawn from present study:

1. Coating layer produced by atmospheric plasma spray process of basalt + SiC powders on AISI 1040 steel pre-coated with Ni + Al5% were comparatively dense and homogeneous. However, coating layer contains some inhomogeneities including porosity and a few semi-melted particles.
2. SiC particles in the microstructure of SiC reinforced basalt base glass–ceramic coating are melted in the plasma flame and oxidized in the atmospheric conditions. But some

unmelted SiC particles can be determined by SEM and EDX analyses.

3. Coated layers of the basalt + SiC powders are generally amorphous which are confirmed by X-ray diffraction patterns, but some crystalline peaks that coming from the unmelted particles.
4. The more the SiC addition resulted to the lower the glass transition temperatures. It is possible that the unmelted SiC particles have the heterogeneous nucleation agent role.
5. The Vickers microhardness results were between 666 and 873 HV_{0.01}. The highest hardness values were observed at %30 SiC additives as expected. It can be appeared that the hardness values generally increase up to 1000 °C. The hardness of the coating layer increases with increasing treatment temperature and SiC addition.
6. The phases formed in the glass–ceramic coating after crystallization heat treatments are includes augite, diopside, albite, andesine and moissanite phases.

Acknowledgements

This work was funded by Sakarya University Research Fund under the contract number 2008-01-08-006. The authors would like to express their gratitude to Sakarya University Engineering Faculty, and Prof. C. Bindal, the head of the Department of Metallurgy and Material Engineering for supporting this work. The authors express their grateful thanks to SENKRON Metal and Ceramic Coating Company of Turkey for performing coatings.

References

- [1] M.G. Rasteiro, T. Gassman, R. Santos, E. Antunes, Crystalline phase characterization of glass–ceramic glazes, *Ceram. Int.* 33 (2007) 345–354.
- [2] E. Bernardo, R. Castellan, S. Hreglich, Sintered glass–ceramics from mixtures of wastes, *Ceram. Int.* 33 (2007) 27–33.
- [3] S. Yılmaz, G. Bayrak, S. Sen, U. Sen, Structural characterization of basalt-based glass–ceramic coatings, *Mater. Des.* 27–10 (2006) 1092–1096.
- [4] G.H. Beall, H.L. Rittler, Basalt glass–ceramics, *Am. Ceram. Soc. Bull.* 55 (1976) 579–582.
- [5] B. Matovic, S. Boskovic, M. Logar, Preparation of basalt-based glass–ceramics, *J. Serb. Chem. Soc.* 68 (2003) 505–510.
- [6] B. Torres, M. Campo, A. Ureña, J. Rams, Thermal spray coatings of highly reinforced aluminium matrix composites with sol–gel silica coated SiC particles, *Surf. Coat. Technol.* 201 (2007) 7552–7559.
- [7] L.H. Cao, K.A. Khor, L. Fu, F. Boey, Plasma spray processing of Al₂O₃/AlN composite powders, *J. Mater. Process. Technol.* 89–90 (1999) 392–398.
- [8] S. Yılmaz, The investigation of production conditions and properties of basalt glass–ceramics materials from the volcanic basalt rocks. Ph.D. Thesis, Istanbul Technical University, Istanbul, 1997.
- [9] A. Akinci, Mechanical and morphological properties of basalt filled polymer matrix composites, *Arch. Mater. Sci. Eng.* 35 (2009) 29–32.
- [10] ASM Handbook, tenth ed., Properties and Selection: Irons, Steels and High Performance Alloys, vol. 1 (2), ASM International, Materials Park, OH 44073, 1990.
- [11] S. Yılmaz, M. Ipek, G. Celebi, C. Bindal, The effect of bond coat on mechanical properties of plasma sprayed Al₂O₃ and Al₂O₃–13 wt%TiO₂ coatings on AISI 316L stainless steel, *Vacuum* 77 (2005) 315–321.
- [12] C. Bartuli, T. Valente, M. Tului, Plasma spray deposition and high temperature characterization of ZrB₂–SiC protective coatings, *Surf. Coat. Technol.* 155 (2002) 260–273.
- [13] V.G. Sevostyanov, E.P. Simonenko, N.T. Kuznetsov, Y.S. Ezhov, Thermodynamic analysis of the production of SiC ceramic via silicon dioxide and

- carbon, in: The Am. Ceram. Soc. Proceedings of the 5th International Conference on High Temperature Ceramic Matrix Composites, 2002, pp. 75–80.
- [14] D.T. Weaver, D.C. Aken, J.D. Smith, The role of bulk nucleation in the formation of crystalline cordierite coatings produced by air plasma spraying, *Mater. Sci. Eng. A* 102 (2003) 339–396.
- [15] J.A. Helsen, J. Proost, J. Schrooten, G. Timmermans, E. Brauns, Glasses and bioglass: synthesis and coatings, *J. Eur. Ceram. Soc.* 17 (1997) 147–152.
- [16] P.W. McMillan, *Glass–Ceramics*, second ed., Academic Press, London, 1979.
- [17] U. Sen, Kinetics of niobium carbide coating produced on AISI 1040 steel by thermo-reactive deposition technique, *Mater. Chem. Phys.* 86 (2004) 189–194.
- [18] J.S. Lee, C.K.H.M.H. Hsu, Y.C. Wu, Kinetic studies on devitrification of calcium phosphate glass with TiO_2 , Al_2O_3 , and SiO_2 additions, *Therm. Acta* 367–368 (2001) 279–283.